

# RESEARCH MEMORANDUM

SOME MEASUREMENTS OF FLYING

QUALITIES OF A DOUGLAS D-558-II RESEARCH AIRPLANE DURING

FLIGHTS TO SUPERSONIC SPEEDS

By Herman O. Ankenbruck and Theodore E. Dahlen

Langley Aeronautical Laboratory Langley Field, Va.

# NATIONAL ADVISORY COMMITTEE FOR AERONAUTICS

WASHINGTON

March 10, 1953 Declassified June 24, 1958

### NATIONAL ADVISORY COMMITTEE FOR AERONAUTICS

#### RESEARCH MEMORANDUM

SOME MEASUREMENTS OF FLYING

QUALITIES OF A DOUGLAS D-558-II RESEARCH AIRPLANE DURING

FLIGHTS TO SUPERSONIC SPEEDS

By Herman O. Ankenbruck and Theodore E. Dahlen

#### SUMMARY

During demonstration flight tests of the air-launched Douglas D-558-II rocket-powered airplane, some measurements of the dynamic lateral stability and lateral and longitudinal trim were obtained in flights up to a Mach number of about 1.87 and to an altitude of about 67,000 feet.

The results indicated that the airplane flying at supersonic speeds in low density air had poor dynamic lateral stability which became more objectionable as Mach number was increased to 1.85. The amplitudes of the oscillations increased as angle of attack decreased. A simplified analysis indicated the directional stability parameter  $c_{n_\beta}$  decreased considerably as Mach number increased from 1.2 to 1.85. With power on and rudder free a lateral oscillation occurred at Mach numbers from 1.1 to 1.4 which did not occur when the rudder was locked. The rudder floating tendency was reversed when power was turned off at the higher supersonic speeds. There were no changes in lateral trim in the transonic region, and the apparent stabilizer effectiveness decreased to about one-third the subsonic value at supersonic speeds.

#### INTRODUCTION

The National Advisory Committee for Aeronautics is conducting research at transonic and supersonic speeds at the NACA High-Speed Flight Research Station at Edwards Air Force Base, Calif., by use of research-type aircraft. One of the aircraft, the Douglas D-558-II (BuAero No. 37974), was recently modified in order to explore the problems of controlled flight in the supersonic speed range. This paper is concerned with this airplane. The modification consisted primarily of an increase in rocket propellant and the use of the airlaunching technique as applied in the X-l project. During the demonstration of the modified aircraft by the Douglas Aircraft Co., attempts to

determine the maximum altitude and Mach number were made, and instrumentation was included to record the conditions of flight during these flights.

Previous data obtained from the airplane before modification (refs. 1 and 2) showed the airplane to have a poorly damped lateral oscillation at low speeds which was difficult to control. Calculations of reference 3 made from limited high-speed data indicated that for the mass, altitude, and speeds expected from the modified airplane, problems of stability and control might be encountered at supersonic speeds.

This paper presents information obtained during the Douglas demonstration flights and has been prepared to show the dynamic behavior of the airplane at supersonic speeds. Also, some information is presented on the variation with Mach number of the aileron and elevator control required for balance. Some aerodynamic-heating measurements obtained in these flights have been presented in reference 4.

#### SYMBOLS

The symbols and coefficients used are defined as follows:

$c_{N_A}$	airplane normal-force coefficient, $\frac{Wn}{qS}$
W	airplane weight, lb
n	normal acceleration, g units
q	free-stream dynamic pressure, $\frac{\rho V^2}{2}$ , lb/sq ft
S	wing area, sq ft
g	acceleration due to gravity, ft/sec2
V	true airspeed, ft/sec
ρ	air density, slugs/cu ft
М	free-stream Mach number
Ъ	wing span, ft
$I_{\mathrm{Z}}$	moment of inertia about the vertical axis, slug-ft2

hp	pressure altitude from standard sea-level conditions, ft
ΔΡ	indicated static pressure minus true static pressure, lb/sq ft
qc'	indicated impact pressure, lb/sq ft
β	angle of sideslip, positive when wind is from the right, deg
p	rolling angular velocity, radians/sec
r	yawing angular velocity, radians/sec
δα	total aileron deflection, $\delta_{a_L}$ - $\delta_{a_R}$ , deg
δe	elevator deflection with respect to the stabilizer surface, deg
it	stabilizer incidence with respect to the fuselage center line, positive when the leading edge is up, deg
δr	rudder deflection, deg
$C_{n_{\beta}}$	static directional stability parameter, rate of change of yawing-moment coefficient with sideslip angle per degree
CZB	dihedral effect, rate of change of rolling-moment coefficient with sideslip angle per degree
$\frac{\text{dit}}{\text{dC}_{N_A}}$	stabilizer effectiveness parameter, stabilizer deflection required to produce a unit change in airplane normal-force coefficient, deg
$c_{ m h_r}$	rudder hinge-moment coefficient, positive clockwise when viewing rudder from top, $\frac{\text{Hinge moment}}{2qM_{\text{l}}}$
Ml	area-moment of rudder, cu ft (3.535 ft <sup>3</sup> )
$c_{h_{\alpha_r}}$	rudder hinge-moment parameter, rate of change of rudder hinge-moment coefficient with sideslip angle per degree $(\alpha = -\beta)$
$\omega_{n}$	undamped natural frequency, cps
t	time, sec

# Subscripts:

L left aileron

R right aileron

#### DESCRIPTION OF THE AIRPLANE

The Douglas D-558-II airplanes were originally constructed to incorporate a combination of turbojet and rocket power. The airplane being used in the present demonstration was modified for air launching and the turbojet engine was removed. Larger tanks were installed to increase the amount of rocket propellants so that a powered flight of approximately 720 cylinder-seconds is possible. The airplane is powered by a four-cylinder rocket engine which utilizes alcohol-water and liquid oxygen and has a design thrust of 1500 pounds per cylinder at sea level.

The D-558-II airplanes have sweptback wing and tail surfaces and are equipped with an adjustable horizontal stabilizer, but no means are provided for trimming out aileron or rudder control forces. No aerodynamic balance or control boost is used in any of the control systems, although hydraulic dampers are provided on all control surfaces to minimize possible control surface "buzz." Dive brakes are located on the rear portion of the fuselage. During some of the flights, a rudder lock was employed. Table I presents pertinent airplane physical characteristics and figure 1 is a three-view drawing of the airplane. Shown in figures 2 and 3 are photographs of the airplane.

#### INSTRUMENTATION AND METHODS

Standard NACA recording instruments are installed in the airplane to measure the following quantities:

Airspeed and altitude
Elevator, stabilizer, left and right aileron, and rudder positions
Angle of attack and sideslip angle
Normal, longitudinal, and lateral accelerations
Pitching, yawing, and rolling angular velocities
Pitching and rolling angular accelerations
Elevator and pedal forces
Aileron wheel force
Rudder hinge moment (one flight only)

A Statham accelerometer was installed at the center of gravity to measure the high-frequency buffeting accelerations. Also recorded were rocket time, radar time, and photopanel frame time. All recording instruments were synchronized by a common timer.

The angle of attack and sideslip angle were measured from vanes mounted on the nose boom at locations of 42 inches and 37 inches, respectively, ahead of the apex of the airplane nose. No corrections to angle of attack or sideslip angle for the upwash or sidewash in front of the airplane at subsonic speeds were made. Also, corrections were not applied for boom bending or pitching velocity.

The position error of the airspeed-altitude system was determined by comparing the static pressure measured in the airplane and the altitude of the airplane measured by radar with the pressure and altitude determined from a radiosonde balloon sent up at the time of each flight.

In the supersonic speed range, the accuracy of the position error calibration is approximately  $\pm 0.01 \frac{\Delta P}{q_c}$ . This gives a possible Mach number error of  $\pm 0.05$  at a Mach number of 1.87.

The airplane weight during flight was estimated from the take-off weight and rocket running time.

# TESTS, RESULTS, AND DISCUSSION

The altitudes for which data are presented vary from 32,000 feet to 67,000 feet for Mach numbers between 0.57 and 1.87. The center-of-gravity location varied from about 27.1 to 26.1 percent of the mean aerodynamic chord. All data are presented for the clean configuration.

# Lateral Stability and Control Characteristics

Previous tests of the airplane at lower speeds (M < 0.87) and calculations made using the best available mass, dimensional, and aerodynamic parameters (refs. 1 to 3) indicated that the dynamic lateral stability might be critically low. In one of the first flights to Mach numbers above 1.0, an uncontrollable lateral oscillation occurred which caused the pilot to terminate the speed run at a Mach number of approximately 1.4. Time histories of measured quantities of Mach number, altitude, normal acceleration, yawing velocity, rolling velocity, rudder and aileron deflection, and sideslip angle obtained during the oscillation are shown in figure 4. Because of the large and violent rudder motion during the oscillation, the rudder was then provided with a

locking device near the control surface. It was found at a later time that the locking device was only partially effective in locking the rudder. Static calibrations with the locking device engaged revealed that rudder movements of  $2\frac{10}{2}$  could be obtained with applied hinge moments of 60 foot-pounds which were the maximum recorded in the flights. The locking device was located in the control system between the rudder and the control position transmitter; hence, there was no indication of rudder movement when the rudder was locked, and hence the rudder positions shown in figures 5 and 6 are only indicated values.

Quantities measured during a flight above a Mach number of 1.0 with the rudder control restrained are shown in figure 5. It is shown that the oscillation previously experienced at Mach numbers less than 1.4 was not present with the control restrained and the Mach number was increased to 1.84. However, as the pilot pushed over to obtain maximum speed in this flight, large lateral oscillations developed which caused the termination of the flight. In these oscillations, sideslip angle reached ±5°, rolling velocity reached ±1.4 radians per second, and bank angles of about ±60° were obtained which were translated to normal-acceleration oscillations of nearly ±1 g having twice the frequency of the lateral oscillation. Deceleration to lower Mach number was accomplished with rocket power off by making a turn to higher lift coefficient. During the oscillations, aileron control was used in an attempt to damp the lateral motion, but did not appear to have any appreciable effect.

In later flights to Mach numbers of 1.87 made at the somewhat higher angles of attack associated with level flight, the same type of oscillation occurred but with considerably less violence. An example of this oscillation is shown in figure 6 where the maximum sideslip was less than 2° and the maximum rolling velocity was about ±0.4 radian per second. This suggests that perhaps changes of some stability derivatives with lift coefficient or the inclination of the principal axis had a considerable influence on the damping of the lateral oscillation.

The values of the directional stability parameter  $c_{n\beta}$  were computed by considering the period of the lateral oscillation, dynamic pressure, and the physical characteristics of the airplane. For an oscillation in one degree of freedom, it can be shown that

$$C_{n_{\beta}} = \frac{4\pi^2 \omega_n^2 I_Z}{57.3qSb}$$

NACA RM L53A06

It is to be noted that the equation is strictly valid only when the effective dihedral is zero which results in a sideslip oscillation with no rolling. For the present case, the rolling motions were large and the simplified formula may be in error. It is believed, however, that the trend of  $c_{n\beta}$  with Mach number might be established by use of the equation.

Data extracted from the flights show that there is a large reduction in the directional stability as Mach number is increased from 1.2 to 1.85. These data are shown in figure 7.

The theoretical values of  $C_{n\beta}$  for the subsonic region were computed from the low-speed wind-tunnel data of reference 5 assuming  $C_{n\beta}$  without tail to be constant at -0.003 per degree and assuming a variation of tail lift-curve slope according to reference 6. The tail contribution in the supersonic region was computed according to references 7 and 8. The tail-off value of  $C_{n\beta}$  was assumed to be constant at -0.0035 per degree, according to unpublished wind-tunnel data obtained recently. The tail-on wind-tunnel test point was also obtained from unpublished data.

Figure 7 shows that the value of  $C_{n\beta}$  decreases from about 0.0037, normally considered in the past to be satisfactory, at a Mach number of 1.2 to about 0.001 at a Mach number of 1.85. As the flight measured values agree with the theory, it can be assumed that the decrease in  $C_{n\beta}$  with Mach number is largely attributable to the decrease in tail lift-curve slope indicated by the theoretical curves. Conditions of the flights were not sufficiently stabilized to determine the damping derivatives or the change in damping of the lateral oscillation, but general inspection of the records indicates that the damping of the lateral oscillation, as might be expected from the predicted decrease in tail lift-curve slope, was reduced with increases in supersonic Mach number. Unpublished high-speed wind-tunnel data indicate that there is also a reduction of  $-C_{l\beta}$  from the values of the low-speed wind-tunnel tests of reference 5; however, the reduction in effective dihedral is not as great as the reduction in static directional stability.

There is reason to believe that low-damped lateral oscillations would result from small disturbances under conditions of low vertical tail effectiveness, high altitudes, and flight at low angles of attack where the effects of principal axis-of-inertia inclination are adverse. As theory indicates that the directional stability will become even less as Mach number is increased further, it is possible that low stability is the major factor limiting the high-speed performance of the airplane in its present configuration.

Presented in figure 8 are hinge-moment data obtained at Mach numbers from 1.65 to 1.85, power on and off, assuming rudder to be rigidly fixed. The values of angle of attack used in obtaining the values of  $C_{h_{\alpha_r}}$  presented in figure 8 are actually the sideslip angles of the airplane as measured by a vane on the boom at the nose of the airplane. The flow angle at the vertical tail is probably not the same as the sideslip angle. The values of  $C_{h_{\alpha_{\mathbf{r}}}}$  presented in figure 8 are intended to show only the changes in the direction and magnitude which occur in going from rocket-off to rocket-on flight. These data show that the rocket operation changed the rudder hinge-moment parameter Char from a negative value of 0.001, power off, to a large positive value of 0.014, power on. The change of character of the rudder motion with power when the rudder was unrestrained is shown clearly in figure 4. At a Mach number of 0.68, values of  $Ch_{\alpha_m}$  on the order of 0.0005 were obtained, power off. For comparison, low-speed wind-tunnel values for similar configurations (ref. 9) are also presented. These wind-tunnel values are presented only for qualitative comparison. As previously pointed out, the airplane sideslip angle is probably not the same as the sideslip angle at the tail. Although it was not possible to obtain consistent data at the intermediate transonic Mach numbers, no effect of power on rudder hinge moments at Mach numbers less than 1.1 was apparent. Measurements of fuselage pressures have shown that rocket exit velocities affect these pressures on the fuselage as far as 2 feet forward of the exit at Mach numbers above 1.0. It is possible, therefore, that by its effects on the rudder hinge moments the rocket exhaust may serve to disturb the airplane and may also have serious effects on the stability and control characteristics. However, sufficient information is not available at present to determine the extent of the effects of underexpansion of the rocket exhaust at high Mach numbers and altitudes.

Earlier tests made with other airplanes in the transonic speed range indicated the possibility that wing-dropping or other lateral trim changes may occur at Mach numbers near 1.0. To keep the wings level on the D-558-II (BuAero No. 37975) airplane, a small amount of aileron was necessary at low subsonic speeds, and at transonic speeds a slight wing-dropping occurred. On the subject airplane (BuAero No. 37974), however, little or no aileron was required to trim at low speeds and no wing-dropping tendencies were apparent in the transonic speed range. Figure 9 is a plot of aileron angle and sideslip angle through the transonic speed range and is typical of five different flights of the all-rocket D-558-II (BuAero No. 37974) airplane. However, in the flights shown in both figure 5 and figure 6, there appeared a directional and lateral trim change at a Mach number near 1.4 as shown by the sideslip angle developed and the aileron deflection used. This occurrence at the same Mach number in two successive flights suggests the possibility

P

that the oscillation was aggravated by, or perhaps started by, a recurrent trim change near a Mach number of 1.4.

# Longitudinal Stability and Control Characteristics

The longitudinal trim data obtained from these flights are rather incomplete as the pilot used elevator and stabilizer interchangeably to trim the airplane. It was therefore impossible to obtain complete elevator trim data through the Mach number range at constant stabilizer angle. The trim curves in figure 10, however, show a trend that was observed in all flights; that is, large nose-down trim changes occurred at Mach numbers from 0.95 to 1.05, then a change in trim occurred in the nose-up direction as the Mach number was increased above 1.1. Above a Mach number of 1.5 increasing up elevator was required for balance with increasing Mach number.

Figure 11 shows the amount of stabilizer needed to produce changes in normal-force coefficient as measured by  $dit/dC_{NA}$ . The wind-tunnel data are from reference 10. The subsonic flight data were obtained from reference 11. No flight data are available at Mach numbers between 0.86 and 1.03; however, it appears that the stabilizer required to create a change in CNA at a Mach number of 1.7 is about three times as great as the low-speed value. As there are no static-longitudinal-stability data in these speed ranges at this time, it is not possible to determine to what extent the increase in the value of  $dit/dC_{N_{\Lambda}}$  is due to an increase in stability or to a decrease in the lift-curve slope of the stabilizer surface.

#### CONCLUSIONS

Results of data obtained in the demonstration flights of the Douglas D-558-II airplane at Mach numbers to about 1.87 and at altitudes to about 67,000 feet indicate the following conclusions:

- 1. At Mach numbers greater than 1.4, an uncontrollable undamped lateral oscillation occurred. The oscillation amplitude appeared to be quite sensitive to changes in angle of attack, larger amplitudes occurring at smaller angles of attack. The dynamic lateral stability characteristics became more objectionable as the Mach number increased to 1.85. A simplified analysis indicates that the directional stability parameter Cng decreased from 0.0037 per degree at a Mach number of 1.2 to
- 0.0010 at a Mach number of 1.85 apparently because of the decrease in vertical-tail lift-curve slope. With power on and the rudder free, an

undamped lateral oscillation occurred between Mach numbers from 1.1 to 1.4, but did not occur when a rudder-locking device was employed; this indicates that the oscillation may have been associated with the floating characteristics of the rudder. At supersonic speeds the direction of the rudder floating tendency was reversed in going from rocket-on to rocket-off flight.

- 2. In flying from subsonic to supersonic speeds little or no measurable change in the aileron deflection required for wings level flight occurred.
- 3. The apparent stabilizer effectiveness in changing normal-force coefficient decreased to about one-third the subsonic value at supersonic speeds. The extent to which this decrease can be attributed to an increase in airplane stability or to a decrease in lift-curve slope of the horizontal tail is not known.

Langley Aeronautical Laboratory,
National Advisory Committee for Aeronautics,
Langley Field, Va.

#### REFERENCES

- 1. Sjoberg, Sigurd A.: Preliminary Measurements of the Dynamic Lateral Stability Characteristics of the Douglas D-558-II (BuAero No. 37974) Airplane. NACA RM L9G18, 1949.
- 2. Stillwell, W. H., and Wilmerding, J. V.: Flight Measurements With the Douglas D-558-II (BuAero No. 37974) Research Airplane. Dynamic Lateral Stability. NACA RM L51C23, 1951.
- 3. Queijo, M. J., and Goodman, Alex: Calculations of the Dynamic Lateral Stability Characteristics of the Douglas D-558-II Airplane in High-Speed Flight for Various Wing Loadings and Altitudes. NACA RM L50H16a, 1950.
- 4. Jones, Ira P., Jr.: Measurements of Aerodynamic Heating Obtained During Demonstration Flight Tests of the Douglas D-558-II Airplane. NACA RM L52I26a, 1952.
- 5. Anon: Preliminary Report on Low-Speed Wind-Tunnel Tests of a 1/4th-Scale Model of the Douglas Model 558, Phase II, Airplane. CWT Rep. 3, Southern Calif. Cooperative Wind Tunnel, May 4, 1948.
- 6. Fisher, Lewis R.: Approximate Corrections for the Effects of Compressibility on the Subsonic Stability Derivatives of Swept Wings. NACA TN 1854, 1949.
- 7. Harmon, Sidney M., and Jeffreys, Isabella: Theoretical Lift and Damping in Roll of Thin Wings With Arbitrary Sweep and Taper at Supersonic Speeds. Supersonic Leading and Trailing Edges. NACA TN 2114, 1950.
- 8. Malvestuto, Frank S., Jr., Margolis, Kenneth, and Ribner, Herbert S.: Theoretical Lift and Damping in Roll at Supersonic Speeds of Thin Sweptback Tapered Wings With Streamwise Tips, Subsonic Leading Edges, and Supersonic Trailing Edges. NACA Rep. 970, 1950. (Supersedes NACA TN 1860.)
- 9. Dods, Jules B., Jr.: Estimation of Low-Speed Lift and Hinge-Moment Parameters for Full-Span Trailing-Edge Flaps on Lifting Surfaces With and Without Sweepback. NACA TN 2288, 1951.
- 10. Osborne, Robert S.: High-Speed Wind-Tunnel Investigation of the Longitudinal Stability and Control Characteristics of a 1/16-Scale Model of the D-558-II Research Airplane at High Subsonic Mach Numbers and at a Mach Number of 1.2. NACA RM L9C04, 1949.

11. Sjoberg, S. A., Peele, James R., and Griffith, John H.: Flight
Measurements With the Douglas D-558-II (BuAero No. 37974) Research
Airplane. Static Longitudinal Stability and Control Characteristics at Mach Numbers up to 0.87. NACA RM L50K13, 1951.

# TABLE I.- PHYSICAL CHARACTERISTICS OF THE

# DOUGLAS D-558-II AIRPLANE

Wing:				
Root airfoil section (normal to 0.30 chord)			. NAC	A 63-010
Tip airfoil section (normal to 0.30 chord)			NACA	631-012
Total area, sq ft				
Span, ft				
Mean aerodynamic chord, in.				
Root chord (parallel to plane of symmetry), in.	•	•		108.51
Tip chord (parallel to plane of symmetry), in	•	•		61.18
Taper ratio				
Aspect ratio		•		3.570
Sweep at 0.30 chord, deg				
Incidence at fuselage center line, deg	•	•		3.0
Dihedral, deg	•	•		-3.0
Geometric twist, deg	•	•		0
Total aileron area (rearward of hinge), sq ft	•	•		9.8
Aileron travel (each), deg	•	•		±15
Total flap area, sq ft				
Flap travel, deg				
Trap draver, deg	•	•		30
**				
Horizontal tail.				
Horizontal tail:  Root sirfoil section (normal to 0.20 shord)			MAC	14 62 010
Root airfoil section (normal to 0.30 chord)				
Root airfoil section (normal to 0.30 chord) Tip airfoil section (normal to 0.30 chord)			. NAC	A 63-010
Root airfoil section (normal to 0.30 chord) Tip airfoil section (normal to 0.30 chord) Area (including fuselage), sq ft			. NAC	A 63-010 39.9
Root airfoil section (normal to 0.30 chord) Tip airfoil section (normal to 0.30 chord) Area (including fuselage), sq ft			. NAC	A 63-010 39.9 143.6
Root airfoil section (normal to 0.30 chord) Tip airfoil section (normal to 0.30 chord) Area (including fuselage), sq ft Span, in. Mean aerodynamic chord, in.			. NAC	A 63-010 39.9 143.6 41.75
Root airfoil section (normal to 0.30 chord) Tip airfoil section (normal to 0.30 chord) Area (including fuselage), sq ft Span, in Mean aerodynamic chord, in. Root chord (parallel to plane of symmetry), in.			. NAC	A 63-010 39.9 143.6 41.75 53.6
Root airfoil section (normal to 0.30 chord) Tip airfoil section (normal to 0.30 chord) Area (including fuselage), sq ft Span, in. Mean aerodynamic chord, in. Root chord (parallel to plane of symmetry), in. Tip chord (parallel to plane of symmetry), in.			. NAC	A 63-010 39.9 143.6 41.75 53.6 26.8
Root airfoil section (normal to 0.30 chord) Tip airfoil section (normal to 0.30 chord) Area (including fuselage), sq ft Span, in. Mean aerodynamic chord, in. Root chord (parallel to plane of symmetry), in. Tip chord (parallel to plane of symmetry), in. Taper ratio			. NAC	A 63-010 39.9 143.6 41.75 53.6 26.8 0.50
Root airfoil section (normal to 0.30 chord) Tip airfoil section (normal to 0.30 chord) Area (including fuselage), sq ft Span, in. Mean aerodynamic chord, in. Root chord (parallel to plane of symmetry), in. Tip chord (parallel to plane of symmetry), in. Taper ratio Aspect ratio			NAC	A 63-010 39.9 143.6 41.75 53.6 26.8 0.50 3.59
Root airfoil section (normal to 0.30 chord) Tip airfoil section (normal to 0.30 chord) Area (including fuselage), sq ft Span, in. Mean aerodynamic chord, in. Root chord (parallel to plane of symmetry), in. Tip chord (parallel to plane of symmetry), in. Taper ratio Aspect ratio Sweep at 0.30 chord line, deg			NAC	A 63-010 39.9 143.6 41.75 53.6 26.8 0.50 3.59 40.0
Root airfoil section (normal to 0.30 chord) Tip airfoil section (normal to 0.30 chord) Area (including fuselage), sq ft Span, in. Mean aerodynamic chord, in. Root chord (parallel to plane of symmetry), in. Tip chord (parallel to plane of symmetry), in. Taper ratio Aspect ratio Sweep at 0.30 chord line, deg Dihedral, deg			NAC	A 63-010 39.9 143.6 41.75 53.6 26.8 0.50 3.59 40.0
Root airfoil section (normal to 0.30 chord) Tip airfoil section (normal to 0.30 chord) Area (including fuselage), sq ft Span, in. Mean aerodynamic chord, in. Root chord (parallel to plane of symmetry), in. Tip chord (parallel to plane of symmetry), in. Taper ratio Aspect ratio Sweep at 0.30 chord line, deg Dihedral, deg Elevator area, sq ft			NAC	A 63-010 39.9 143.6 41.75 53.6 26.8 0.50 3.59 40.0
Root airfoil section (normal to 0.30 chord) Tip airfoil section (normal to 0.30 chord) Area (including fuselage), sq ft Span, in.  Mean aerodynamic chord, in. Root chord (parallel to plane of symmetry), in. Tip chord (parallel to plane of symmetry), in. Taper ratio Aspect ratio Sweep at 0.30 chord line, deg Dihedral, deg Elevator area, sq ft Elevator travel, deg			NAC	A 63-010 39.9 143.6 41.75 53.6 26.8 0.50 3.59 40.0 0
Root airfoil section (normal to 0.30 chord) Tip airfoil section (normal to 0.30 chord) Area (including fuselage), sq ft Span, in. Mean aerodynamic chord, in. Root chord (parallel to plane of symmetry), in. Tip chord (parallel to plane of symmetry), in. Taper ratio Aspect ratio Sweep at 0.30 chord line, deg Dihedral, deg Elevator area, sq ft Elevator travel, deg Up			NAC	A 63-010 39.9 143.6 41.75 53.6 26.8 0.50 3.59 40.0 0 9.4
Root airfoil section (normal to 0.30 chord) Tip airfoil section (normal to 0.30 chord) Area (including fuselage), sq ft Span, in.  Mean aerodynamic chord, in. Root chord (parallel to plane of symmetry), in. Tip chord (parallel to plane of symmetry), in. Taper ratio Aspect ratio Sweep at 0.30 chord line, deg Dihedral, deg Elevator area, sq ft Elevator travel, deg Up Down			NAC	A 63-010 39.9 143.6 41.75 53.6 26.8 0.50 3.59 40.0 0 9.4
Root airfoil section (normal to 0.30 chord) Tip airfoil section (normal to 0.30 chord) Area (including fuselage), sq ft Span, in.  Mean aerodynamic chord, in. Root chord (parallel to plane of symmetry), in. Tip chord (parallel to plane of symmetry), in. Taper ratio Aspect ratio Sweep at 0.30 chord line, deg Dihedral, deg Elevator area, sq ft Elevator travel, deg Up Down Stabilizer travel, deg			NAC	A 63-010 39.9 143.6 41.75 53.6 26.8 0.50 3.59 40.0 0 9.4
Root airfoil section (normal to 0.30 chord) Tip airfoil section (normal to 0.30 chord) Area (including fuselage), sq ft Span, in. Mean aerodynamic chord, in. Root chord (parallel to plane of symmetry), in. Tip chord (parallel to plane of symmetry), in. Taper ratio Aspect ratio Sweep at 0.30 chord line, deg Dihedral, deg Elevator area, sq ft Elevator travel, deg Up Down Stabilizer travel, deg Leading edge up			NAC	A 63-010 39.9 143.6 41.75 53.6 26.8 0.50 3.59 40.0 0 9.4
Root airfoil section (normal to 0.30 chord) Tip airfoil section (normal to 0.30 chord) Area (including fuselage), sq ft Span, in.  Mean aerodynamic chord, in. Root chord (parallel to plane of symmetry), in. Tip chord (parallel to plane of symmetry), in. Taper ratio Aspect ratio Sweep at 0.30 chord line, deg Dihedral, deg Elevator area, sq ft Elevator travel, deg Up Down Stabilizer travel, deg			NAC	A 63-010 39.9 143.6 41.75 53.6 26.8 0.50 3.59 40.0 0 9.4

# TABLE I.- PHYSICAL CHARACTERISTICS OF THE

# DOUGLAS D-558-II AIRPLANE - Concluded

Vertical tail:
Airfoil section (normal to 0.30 chord)
Fuselage:
Length, ft       42.0         Maximum diameter, in       60.0         Fineness ratio       8.40         Speed-retarder area, sq ft       5.25
Power plant:
Rocket
Airplane weight (full rocket fuel), lb
Airplane weight (no fuel), lb 9,421
Center-of-gravity locations: Full rocket fuel (gear up), percent mean aerodynamic chord
Moments of inertia (no fuel): About normal axis, slug-ft <sup>2</sup>

NACA

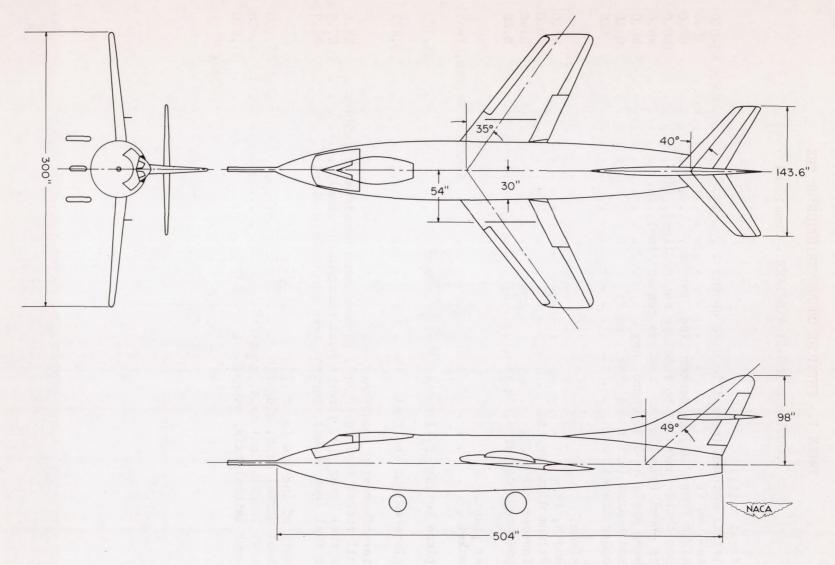


Figure 1.- Three-view drawing of the Douglas D-558-II research airplane.

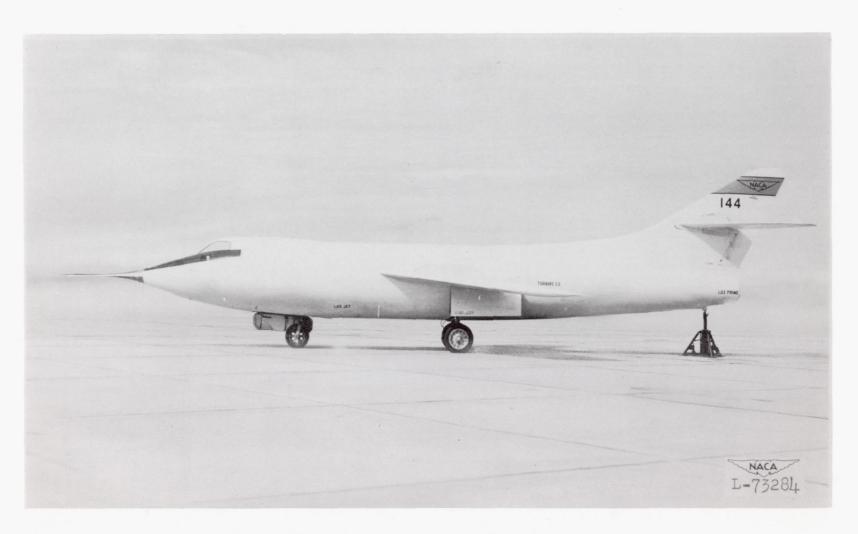


Figure 2.- Side view of Douglas D-558-II research airplane.

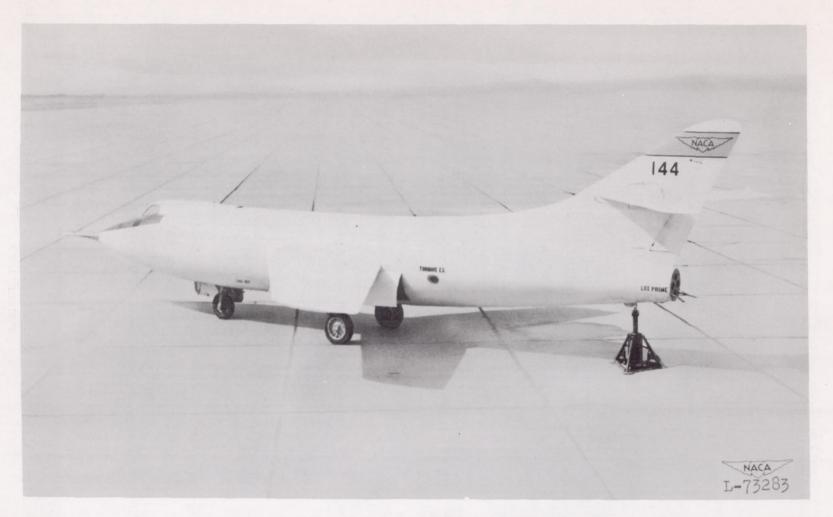


Figure 3.- Three-quarter rear view of Douglas D-558-II research airplane.

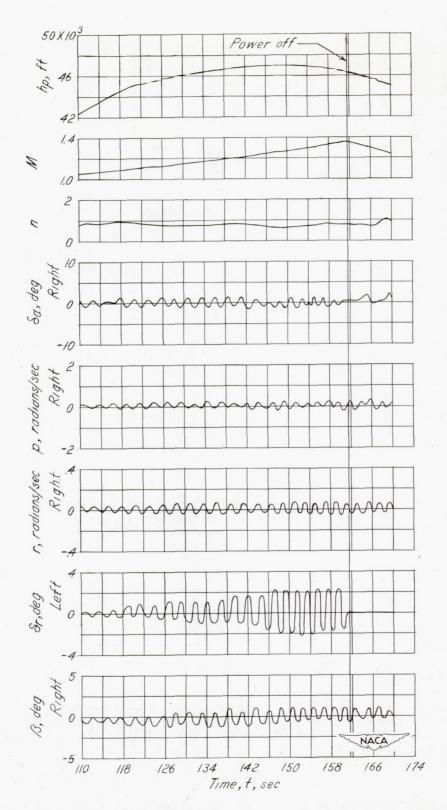


Figure 4.- Time history of lateral oscillation at supersonic speeds without rudder lock.

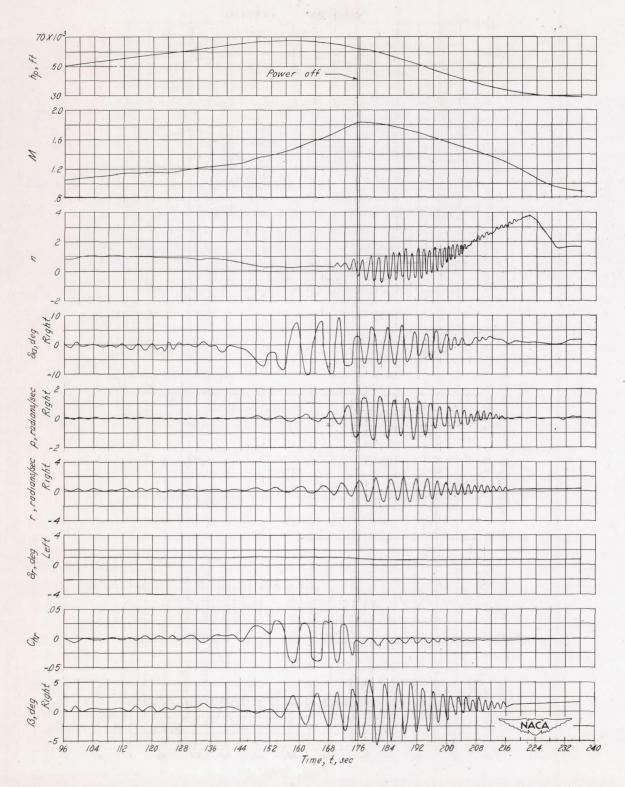


Figure 5.- Time history of a lateral oscillation at supersonic speeds with rudder restrained. Low acceleration push-over.

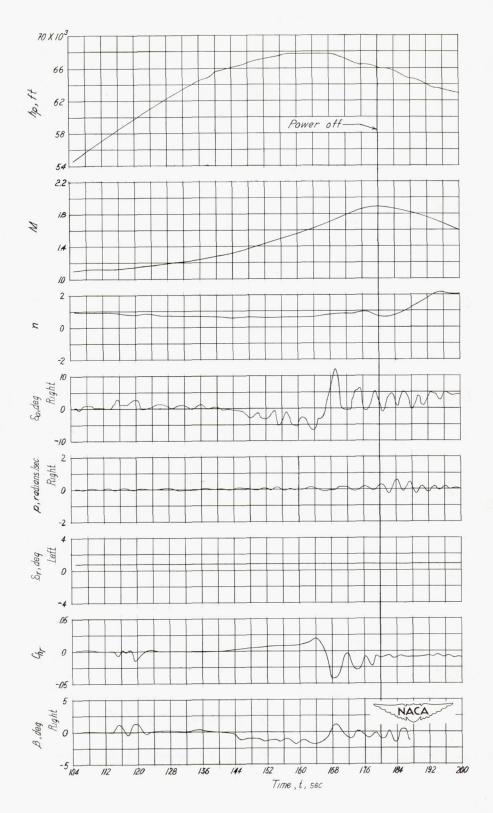
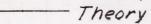


Figure 6.- Time history of a lateral oscillation at supersonic speeds with rudder restrained. Moderate acceleration push-over.

- o Flight
- D Wind tunnel, Vertical tail on
- Wind tunnel, Vertical tail off



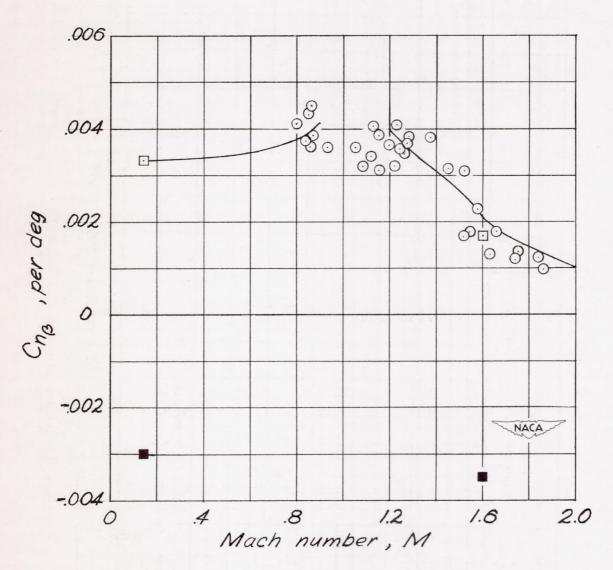


Figure 7.- Static directional stability as measured in lateral oscillations.

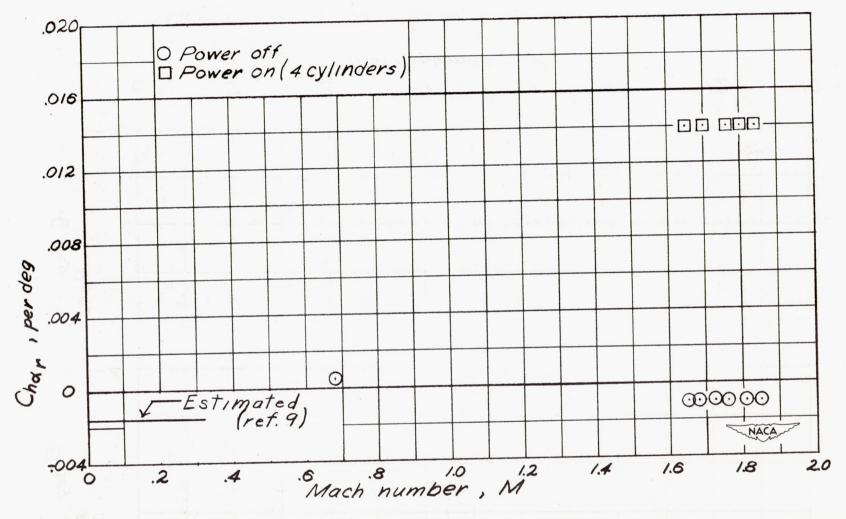


Figure 8.- Rudder hinge-moment parameter  $C_{\mathbf{h}_{\alpha_{\mathbf{r}}}}$  power on and off.

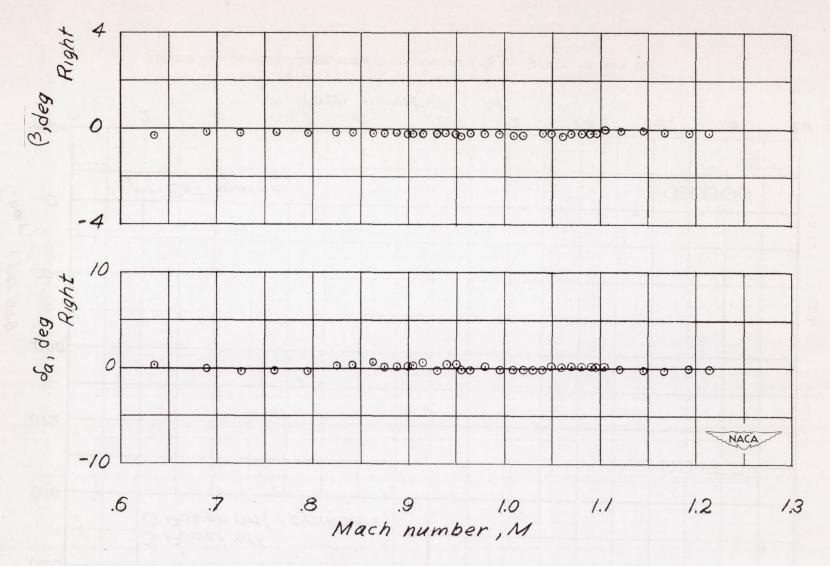


Figure 9.- Aileron position and sideslip angle through the transonic region with rudder locked.

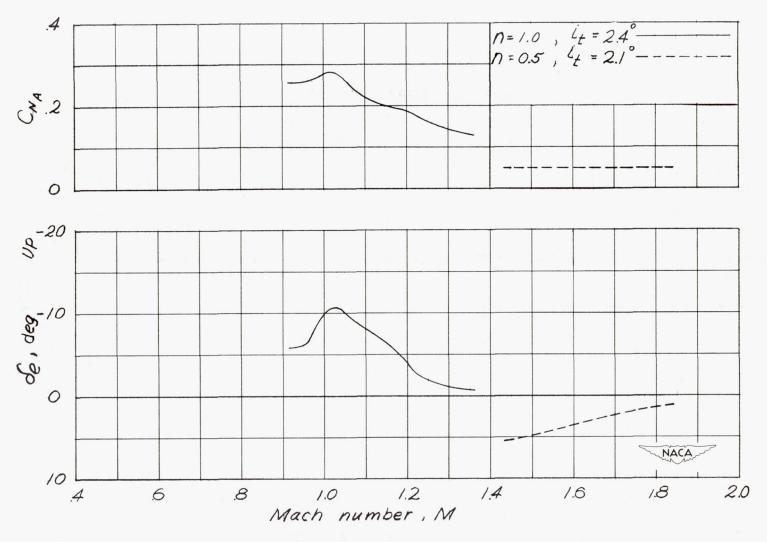


Figure 10.- Examples of elevator deflection required to trim obtained during flights to supersonic speeds.

P

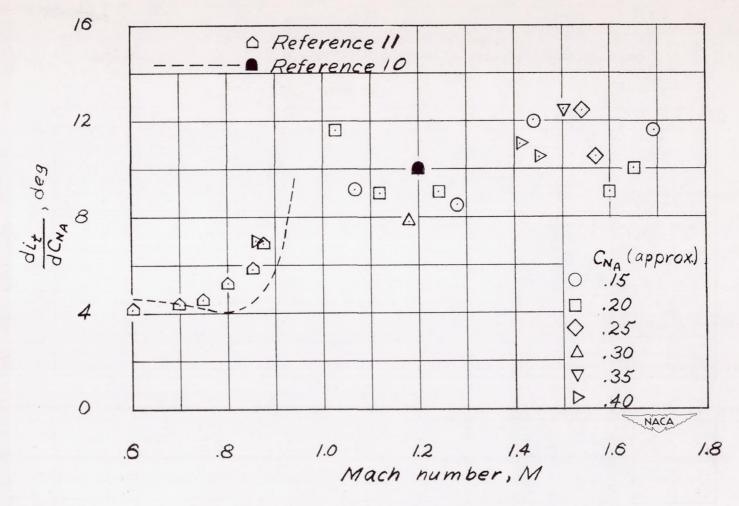


Figure 11.- Apparent stabilizer effectiveness.